RESEARCH PAPER

Impact of the functionalization of janus MnO_2 nanomaterials on the kinetic of the catalytic asphaltene oxidation

P.A. Rivera-Quintero [a], D. Fabio Mercado [a,b,*], Hernando Guerrero-Amaya [a], Luz M. Ballesteros-Rueda [a]

[a] Centro de Investigaciones en Catálisis (@CICAT UIS), Parque Tecnológico Guatiguará (PTG), Universidad Industrial de Santander, Km. 2 vía El Refugio, Colombia
[b] Grenoble INP, LMGP, Institute of Engineering, Université Grenoble Alpes, 38000 Grenoble, France

Abstract

Due to the increasing energy demand and the depletion of light crude oil, the exploitation of heavy crude oil fields is being considered as an alternative. In-situ combustion is an enhanced oil recovery thermal technique that involves injecting air or oxygen into the well to promote partial oxidation of the oil. However, the initial ignition of combustion has posed significant challenges. Therefore, special attention must be given to low-temperature oxidation. Furthermore, asphaltenes contribute to coke formation as a fuel. Janus nanomaterials catalysts can be utilized to lower the ignition temperature. In this study, we focused on investigating the catalytic oxidation of asphaltenes primarily in the low-temperature oxidation region. To achieve the research objective, the catalytic oxidation of asphaltenes was studied using janus-functionalized MnO_2 nanoparticles that were previously synthesized and characterized using both adipic and hexanoic acid. It was observed that surface functionalization reduces the exothermic nature of the process, and the apparent activation energies for the functionalized materials are lower than those for the virgin asphaltenes and the obtained MnO_2, thus demonstrating their catalytic activity. Additionally, the stability of the formed nanofluids is maintained for up to 24 h.

Keywords: Asphaltene, Colloid transport, In-situ combustion, Janus nanomaterials, MnO_2

1. Introduction

Due to the depletion of conventional light oils, the growth in energy demand, and the high prices of crude oil, there is an urgent need to exploit alternative fossil resources. In this regard, increasing the recovery factor through enhanced oil recovery processes is of special interest.[1,2] In-situ combustion (ISC) involves injecting atmospheric air or oxygen-enriched gas into the well to promote the partial oxidation of the oil.[3,4] When the reservoir temperature provides sufficient energy for oxidation reactions, an ignition region is enhanced. Due to ignition and reaction in place, the ISC front moves through the reservoir, leading to the mobilization of unburned oil out of the reservoir and through the production well.[5] Despite recent studies on ISC, there is still insufficient knowledge about the process due to the complexity of hydrocarbon mixtures and their chemical reactions. Therefore, individual fractions of crude oil, such as saturates, aromatics, resin, and asphaltenes, have been studied.[6] This investigation focuses on analyzing asphaltenes as a representative fraction of crude oil.

In the context of ISC, three main oxidation regimes are proposed, namely low-temperature oxidation (LTO), typically up to 300 °C, fuel deposition between 300 and 450 °C, and high-temperature oxidation (HTO) above 450 °C.[7] For heavy oil deposits, the products of LTO reactions are essential

Received 15 February 2023; revised 4 December 2023; accepted 12 December 2023.
Available online 8 April 2024

* Corresponding author at: Industrial University of Santander, Grenoble, Auvergne-Rhône-Alpes, France.
E-mail addresses: dfabiomercado@gmail.com, dfmercad@unal.edu.co (D. Fabio Mercado).

https://doi.org/10.62593/2090-2468.1004

for maintaining the combustion front. However, achieving successful production during the initial ignition remains a significant challenge for the ISC process. On the other hand, asphaltenes, among other individual fractions, contribute significantly to the formation of coke as fuel. Asphaltenes are a portion of oil that exhibits insolubility in low molecular weight n-paraffin solvents but solubility in light aromatic hydrocarbons. They are characterized by their structural composition, featuring polyaromatic cores linked to aliphatic chains that incorporate different heteroatoms.[8]

The use of catalysts has been proposed to address these challenges, as they can improve the ignition success rate and establish a self-sustaining combustion front.[9] In addition to stability improving of the combustion front, catalysts can also decrease the activation energy of crude oil oxidation reactions, leading to a reduction in the ignition temperature.[10] Varfolomeev et al.[9] and Golafshani et al.[11] studied the catalytic oxidation of heavy oil mediated by transition metal-based acetylacetonates. They calculated the activation energy using different isoconversional methods and concluded that the presence of metal decreased the oxidation temperature for both fuel deposition and HTO. Nevertheless, to achieve desirable reaction yields, a relatively high dosage of catalysts with small particle sizes is a promising option, making the use of nanomaterials a suitable solution.[12] Furthermore, nanomaterials possess unique properties due to their small size and large surface area per unit volume. In heterogeneous catalytic processes, reactions occur on the surfaces of nanomaterials, and their affinity with water/oil phases must always be considered to achieve optimal catalytic performance during the ISC combustion process.[13] Nevertheless, the utilization of nanomaterials in reservoirs faces challenges associated with transport limitations arising from their lipophilic nature. Therefore, it is essential to ensure that the catalytic solids form stable nanofluids, guaranteeing smooth transportation through the injection well.[14]

In previous studies, Mercado et al.[15] synthesized five transition metal oxides in the asphaltene oxidation process, among which Fe_2O_3, MnO_2, and MoO_3 decreased the asphaltene oxidation temperature in the LTO region. Additionally, Quintero et al.[16] synthesized janus-type nanomaterials (JNM) for different crystalline phases of MnO_2, using APTES and citric acid as functionalizing agents, where Janus are amphiphilic materials (the name was taken from the double sides of Roman God). These JNMs have a different chemical identity on each face due to the selection of functionalization agents. The study concluded that while APTES decreased the LTO temperature, the use of citric acid improved the stability of MnO_2 nanofluids. The challenge, therefore, lies in injecting amphiphilic catalysts into the reservoir through the porous medium and examining their catalytic activity on heavy oil oxidation. Recently, Shi et al.[17] studied the applicability of JNM in nanofluids for oil displacement systems in low-permeability reservoirs. However, although surface functionalization has been proposed to stabilize nanofluids, the impact of functionalization on the kinetic of catalytic oxidation of heavy oils has not yet been reported, and this is a critical parameter for the ISC process. Among the functionalization agents, adipic acid (AA) and hexanoic acid (HA) have strong potential for functionalization due to the presence of −COOH polar groups within a nonpolar carbon backbone.[18]

However, an extensive examination of recent literature leads to the conclusion that the evaluation of impact of organic functionalization on the reaction kinetics of asphaltene oxidation has not been reported yet, and its behavior is still unknown. Therefore, the objective of this research is to evaluate the effect of anisotropic functionalization of JNM based on MnO_2 functionalized with adipic and hexanoic acid on the activation energy of the catalytic oxidation of asphaltenes in the LTO region using the Ozawa–Flynn–Wall (OFW) method.

2. Materials and methods

2.1. Materials

Manganese II sulfate monohydrate ($MnSO_4 \cdot H_2O$) 97% wt. and ammonium persulfate ($(NH_4)_2S_2O_8$) 98% wt. were supplied by Panreac. Absolute ethanol 99%, hexadecyltrimethylammonium bromide (CTAB) 98%wt., hexanoic acid more than or equal to 98%, dichloromethane, sodium hydroxide 99% wt. and sodium nitrate ($NaNO_3$) 99.5% wt., were provided by Sigma Aldrich (Saint Louis, MO, United States). Adipic acid 99%wt. and paraffin (21–53 °C) were obtained from Carlo Erba. All reagents were used without further purification. Deionized water (18 MΩ cm at 25 °C) was used.

2.2. Methods

2.2.1. Synthesis of β-MnO_2 and characterization

The synthesis procedure and physicochemical properties of MnO_2 used in this study are based on the procedure and characterization methods previously achieved by Quintero et al..[16] The produced

MnO_2 powder was analyzed for TEM, XPS, FTIR, thermogravimetric analyses (TGA), and XRD tests.

2.2.2. Functionalization of MnO_2 nanomaterials

Anisotropic functionalization was performed following the methodology as previously described.[16] In this study, using the Pickering emulsion methodology, adipic acid (AA) and hexanoic acid (HA) were used as functionalizing agents at a ratio of 0.016 mol −COOH/g MnO_2 for both agents.

In summary, for achieving the functionalization, a certain amount of functionalizing agent dissolved in a 0.5 M NaOH basic solution with a pH = 10 higher than the pK_a of the carboxylic acids (pK_a adipic acid = 4.42 and 5.42, pK_a hexanoic acid = 4.88) was added to an emulsion containing wax and MnO_2 dispersed in an ethanol-aqueous solution (6.7% w/w ethanol/water).

The mixture was stirred at 750 rpm for 24 h. After 24 h, solid wax microspheres with MnO_2 nanomaterials on the surface were precipitated and separated by centrifugation at 3000 rpm for 10 min. The solid materials were washed with dichloromethane and ethanol to dissolve the wax and remove physiosorbed organic agents and other contaminants. Subsequently, the functionalized nanomaterials were dried in an oven at 60 °C for 2 h. The resulting materials were labeled as MnO_2@HA and MnO_2@AA according to their functionalizing agent, being hexanoic acid and adipic acid, respectively. This methodology is illustrated in Figure S1 (https://ejp.researchcommons.org/cgi/viewcontent.cgi?filename=0&article=1004&context=journal&type=additional&preview_mode=1).

2.2.3. Preparation of the aqueous suspensions with nanomaterials

Aqueous suspensions of the nanomaterials were synthesized by suspending the solids in water at a concentration of 100 ppm. The suspensions were then sonicated in an ultrasonic bath for 30 min with a power of 200 W. The suspensions were labeled as MnO_2, MnO_2@AA, and MnO_2@HA, corresponding to each nanomaterial.

The stability of the aqueous suspensions was evaluated by measuring the zeta potential of the agglomerates using the dynamic light scattering technique. This was carried out using a LiteSizer500 particle analyzer by Anton Paar. Additionally, photographs of the suspensions were taken with a 12 MP camera (Fig. 2b) at hourly intervals for a duration of 1 day to observe any changes in their appearance.

2.2.4. Asphaltenes oxidation catalyzed by janus MnO_2 nanomaterials

The extraction of asphaltenes and the impregnation of the nanomaterials was achieved following a previously reported protocol.[16] To impregnate the materials, a known quantity of asphaltenes was brought into contact with 0.05 g of each nanomaterial, ensuring a mass ratio of 70/30 for nanomaterials and asphaltenes, respectively, in all cases. The impregnated material was then analyzed using a DSC 250 equipment (TA instruments). The DSC analysis was conducted in the temperature range of 30–450 °C. The experiment started with an initial equilibration time of 5 min, followed by a heating ramp of 10 °C/min under a flow of 50 ml/min of air.

2.2.5. Study the kinetic of asphaltene catalytic oxidation process

In order to study the catalytic oxidation of asphaltenes impregnated with the nanomaterials, TGA were performed on a discovery thermogravimetric analyzer (TA Instruments), heating a 10 mg sample under an air flow at 25 ml/min from 50 to 550 °C with an initial and final equilibration time of 5 min, with different heating ramps (η = 1, 5, 7, 10, 15 °C/min). The activation energy (E_α) was estimated using the isoconversional OFW method.[11] OFW method is proposed as follows in Equation (1):

$$log\,(\eta) = log\left(\frac{K_\alpha E_\alpha}{Rg(\alpha)}\right) - 2.315 - 0.4567\frac{E_\alpha}{RT} \tag{1}$$

Where, η is the temperature ramp (°C/min), K_α is the pre-exponential factor (1/s), E_α is the activation energy (kJ/mol), R is the ideal gas constant (8314 J/K mol), g(α) is based on a function that describes asphaltene conversion, and T is the reaction temperature (K). The conversion ratio (α) was calculated from the mass loss data according to Equation (2):[16]

$$\alpha = \frac{(m_0 - m_T)}{(m_0 - m_\infty)} \tag{2}$$

And g(α) is defined by Equation (3):

$$g(\alpha) = \int_0^\alpha \frac{d\alpha}{f(\alpha)} = \int_0^T \frac{K_\alpha\, exp\left(-\frac{E_\alpha}{RT}\right)}{\eta} dT \tag{3}$$

Where, m_0 is the mass of the initial sample (at T = 50 °C), m_∞ is the mass of the final sample (at T = 550 °C) and m_T is the mass of the sample at a given temperature (T).

3. Analysis and discussion of results

3.1. Characteristics of the synthesized MnO_2

The physicochemical properties of MnO_2 are detailed in depth in a previous work and in the Supporting Information Files.[16] In summary, according to the results of XPS, FTIR, and TGA, the synthesis was satisfactory and resulted in a black powder that corresponds to a metal oxide core with a surface layer of -MnOH.

The material exhibited low hydrophilicity and lacked stability in aqueous suspensions. XRD analysis confirmed the formation of MnO_2 nanomaterials in the pyrolusite structure (β-MnO_2), without the presence of mixed crystalline phases (Figure S2 (https://ejp.researchcommons.org/cgi/viewcontent.cgi?filename=0&article=1004&context=journal&type=additional&preview_mode=1)). These nanomaterials displayed a nanorod-like morphology, with an average diameter of 34 ± 18 nm and a length of 873 ± 333 nm (Figure S3 (https://ejp.researchcommons.org/cgi/viewcontent.cgi?filename=0&article=1004&context=journal&type=additional&preview_mode=1)).

3.2. Characteristics of anisotropic functionalization

3.2.1. FTIR spectrum

The attenuated total reflectance FTIR method employed to record the spectra in Figure S4 (https://ejp.researchcommons.org/cgi/viewcontent.cgi?filename=0&article=1004&context=journal&type=additional&preview_mode=1) is mostly sensitive to functional groups very near the particle surfaces.[19] All samples exhibit bands in the range of 800–400 cm^{-1}, attributed to the stretching vibration modes of Mn–O and Mn–O–Mn groups.[16] The presence of O–H groups belonging to adsorbed water and Mn–OH surface groups is evidenced by the bands between 3200 and 3600 cm^{-1}, 1628 and 1075 cm^{-1}. In the case of free AH and AA, the typical signals of $-CH_3$ are observed around 2945 and 2920 cm^{-1}, respectively.

Additionally, strong absorption bands at 1682 and 1705 cm^{-1} are observed for AA and AH, respectively, indicating the presence of the –COOH group. However, in the case of functionalized materials, these bands are noticeable at 1563 cm^{-1}, suggesting an interaction of this group with the metal oxide nanomaterial. Interestingly, no contribution from free –COOH groups is observed for MnO_2@HA. However, for MnO_2@AA, a minor signal at 1653 cm^{-1} supports the presence of free –COOH surface groups. Therefore, in the case of MnO_2@AA, a fraction of AA molecules is adsorbed on the surface through both –COOH groups, while some interact only with one of the carboxylic acid groups.

3.2.2. Thermogravimetric analyses analysis

Fig. 1 presents the thermograms of all samples obtained from TGA analysis. A mass loss of ~0.64% is observed for MnO_2 between 100 and 200 °C, which is attributed to the presence of physisorbed and chemisorbed water molecules. Another mass

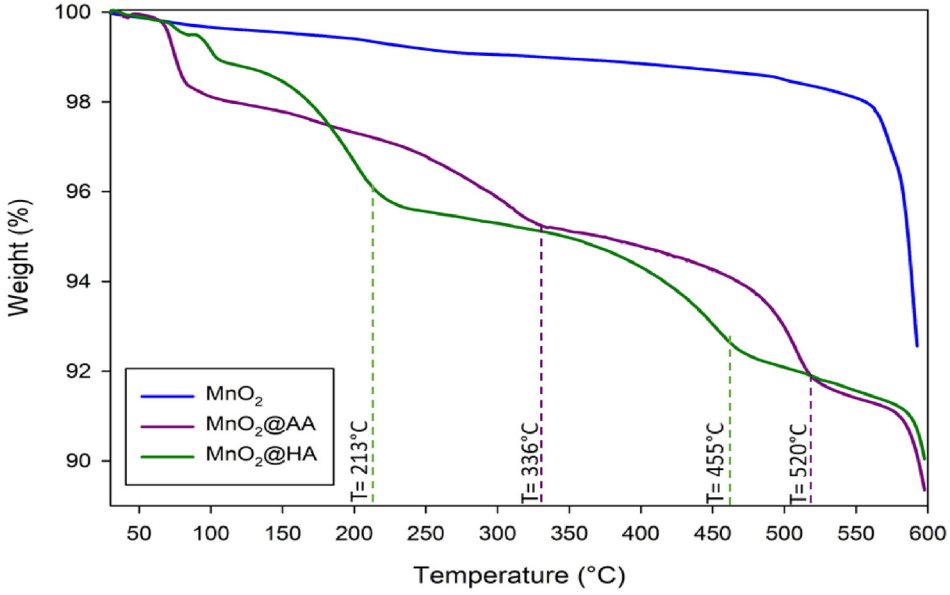

Fig. 1. Thermogravimetric profile of samples MnO_2, MnO_2@HA, and MnO_2@AA.

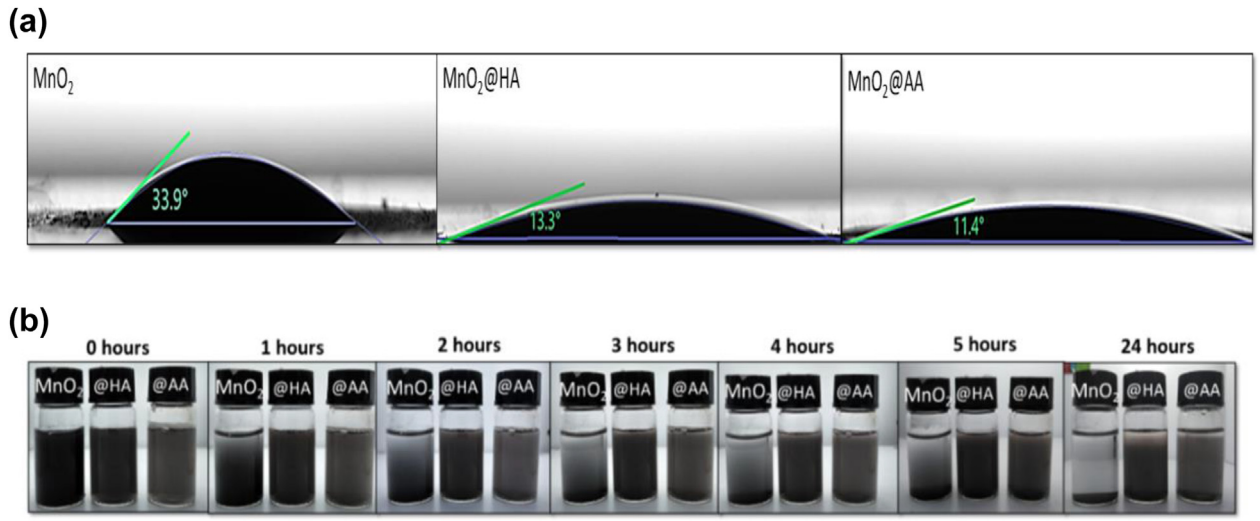

Fig. 2. Image of the static contact angle (SCA) between a drop of water and (a) MnO_2 $\theta = 33.9 \pm 2.0°$, (b) MnO_2@HA $\theta = 13.3 \pm 1.7°$, (c) MnO_2@AA $\theta = 11.4 \pm 1.9°$, (b) image of 100 ppm aqueous suspension after 24 h.

loss of 0.71% occurring between 200 and 500 °C is assigned to the dehydroxylation of Mn−OH surface groups. The significant mass loss observed above 500 °C is attributed to the reduction of MnO_2 to Mn_2O_3, accompanied by the evolution of molecular oxygen.

In summary, the results presented above indicate the successful synthesis of janus-type MnO_2-based nanomaterials. The functionalization agents are adsorbed on the surface of MnO_2, imparting the material with an anisotropic chemical functionality, primarily contributed by the −COOH groups.

MnO_2@HA and MnO_2@AA exhibit a considerable mass loss, which is attributable to the surface functionalization with the corresponding organic molecule. The reported boiling points for HA and AA are 204 ± 4 and 337 ± 15 °C at 1 atm, respectively, and at these temperatures mass losses of 2.74 and 3.24% are appreciable. These results suggest that a fraction of the corresponding organic acid is physisorbed on the surface, possibly due to hydrogen bonding between the −COOH group and the Mn−OH surface group, leading to the formation of metal-organic complexes between negatively charged -COO^- groups and Mn^{+4} or Mn^{+3} cations on the surface. Furthermore, nonpolar intermolecular forces due to the carbon backbone are not observed.

An additional mass loss of 3.45 and 3.41% are observed in the temperature range between the corresponding boiling point of the organic acid and 455 or 520 °C, for MnO_2@HA or MnO_2@AA, respectively. These results indicate the chemisorption of a fraction of the respective organic acid onto the surface.

The total adsorbed moles of the corresponding organic acid per gram of MnO_2, calculated trough the TGA results, are 0.52 with 55% of chemisorbed moles for MnO_2@HA and 0.47 mmol with 52% of chemisorbed moles for MnO_2@AA. Therefore, it can be inferred that the number of carboxylic groups adsorbed with both functionalizing agents is approximately the same which is consistent with what was observed in FTIR, where the signal shift due to functionalization is also very similar.

3.2.3. Static contact angles analysis

Fig. 2a shows a series of photographs in which the static contact angles (SCA) in an air atmosphere, using water are 33.9 ± 2.0°, 13.3 ± 1.7°, and 11.4 ± 1.9° for MnO_2, MnO_2@HA, and MnO_2@AA, respectively. These photographs suggest that the functionalization with the organic acids increases the hydrophilicity of the nanomaterial. This behavior can be attributed to the proposed H-bonding between water molecules and the −COOH group. Interestingly, the MnO_2@HA material demonstrates augmented hydrophilicity, implying the existence of surface-exposed free −COOH groups.

3.3. Aqueous suspensions with nanomaterials

3.3.1. Dynamic light scattering analysis

The electrophoretic mobility values, measuring 0.17 ± 0.01 μm cm/Vs, for 10 ppm aqueous suspensions of MnO_2 (pH = 7.1), are noteworthy. However, upon functionalization these values increase up to 0.30 ± 0.02 and 0.43 ± 0.01 μm cm/Vs in absolute value, for MnO_2@HA (pH = 6.5) and

MnO_2@AA (pH = 7.5), respectively. A similar trend of strongly marked negative values in the presence of −COOH groups was reported by Penelas et al..[20] The functionalized nanomaterials, where some hydroxyl −OH groups were replaced by organic acid, exhibit higher electrophoretic mobility compared to MnO_2.

3.3.2. Stability

These results are coherent with the SCA photographs, demonstrates an increase in the hydrophilicity. The kinetic behavior of the suspension of the materials in water was also investigated, as shown in Fig. 2b. It is shown that suspension with MnO_2 fully settled within 8 h, whereas the functionalized samples remained suspended for 24 h. This observation agrees with the SCA and electrophoretic mobility results.

3.4. Asphaltenes oxidation catalyzed by MnO_2 nanomaterials

3.4.1. Effect of functionalization agent on the kinetic of the oxidation process

Fig. 3 shows the conversion ratio (α) versus temperature for the virgin asphaltenes and with nanomaterials dispersed on them. It is evident that α is higher at any given temperature below 480 °C. For instance, at 350 °C, α has values of 0.20, 0.25, and 0.32, for MnO_2@HA, MnO_2, and MnO_2@AA and, respectively, while at that same temperature the virgin asphaltenes barely reach a conversion of 0.07. These results indicate that all three nanosolids promote the oxidation of asphaltenes and act as (nano)catalysts for asphaltene oxidation in an air-saturated atmosphere, particularly at temperatures below 480 °C. The shift of the reaction regions towards lower temperatures can be attributed to the redox properties of the oxide structure.[21] In fact, in a previous study[16] it was shown that the crystalline phase of MnO_2 and the organic functionalizing agent impact the thermal behavior of asphaltene oxidation. Additionally, furthermore, all the MnO_2-based materials evaluated catalyzed asphaltene oxidation. In that regard, the LTO oxidation regimen is catalyzed by the material. Moreover, it is evident that the functionalization agent impacts the catalytic activity of the obtained materials. Above 500 °C, an apparent non-catalytic effect may be observed due to the reduction of MnO_2 to Mn_3O_4 (*vide supra*).

In order to thoroughly analyze the effect of the functionalization agent on the kinetic of the oxidation process, the rate of mass loss (DTG) as a function of temperature for the virgin and the nanocatalyst containing asphaltenes were obtained as evidenced in Fig. 4. The DTG curves for pure asphaltenes exhibit a single prominent peak between 310 and 550 °C, corresponding to the temperature range in which noncatalytic asphaltene oxidation occurs.[22] However, different behaviors are

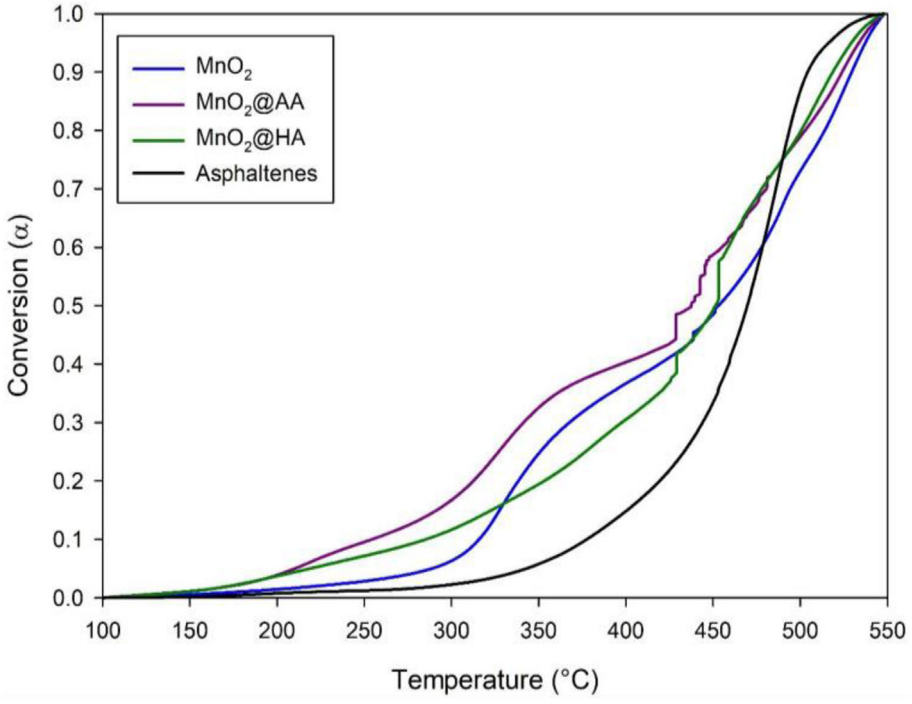

Fig. 3. Conversion ratio of virgin asphaltenes and asphaltenes with nanomaterial dispersion.

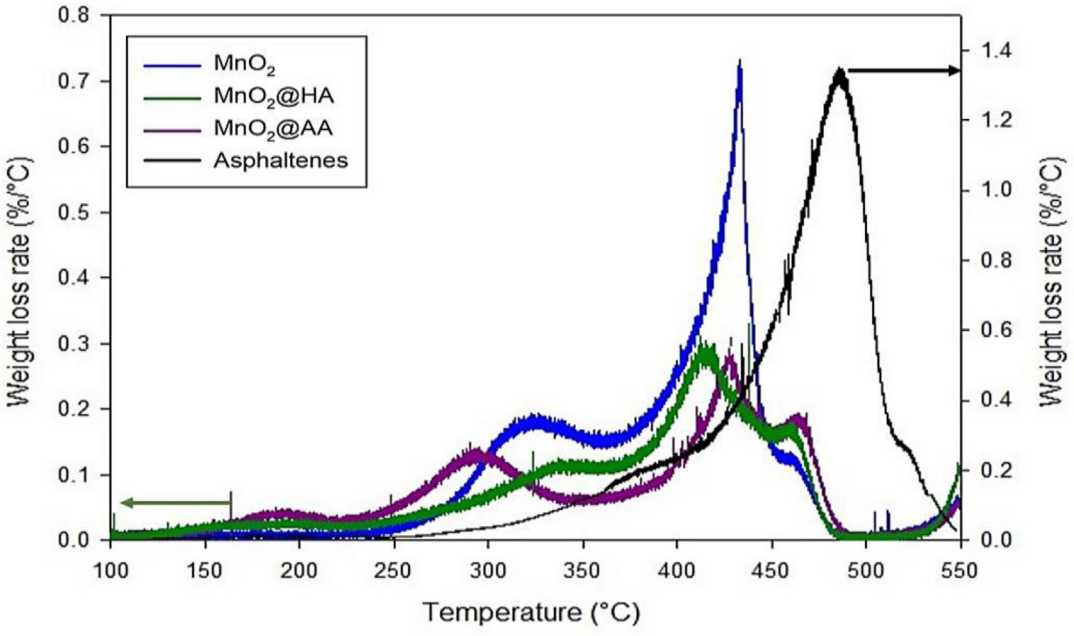

Fig. 4. Rate of mass loss as a function of temperature (DTG) at heating rate of 7 °C/min.

appreciable in this range. A relatively low mass loss rate is appreciated below 350 °C which corresponds to LTO regimen. A shoulder around 375 °C suggests the presence of an additional oxidation regimen which could be attributed to the intermediate oxidation temperature (ITO) or fuel deposition. Above this temperature, a substantial increase in mass loss is observed, which can be attributed to thermal cracking or pyrolysis. The global maximum temperature at 488 °C corresponds to the HTO regime, in which complete oxidation takes place accompanied by the formation of gases such as CO_2 and H_2O.

Upon the introduction of the nanocatalysts, the DTG profiles showed different behavior. The most evident modification is that the peaks shift to lower temperatures, that is at least 50 °C, which is coherent with the TGA results of the asphaltenes (Figure S5a (https://ejp.researchcommons.org/cgi/viewcontent.cgi?filename=0&article=1004&context=journal&type=additional&preview_mode=1)) where the catalytic activity was evidenced. For MnO_2, the profile exhibits similar features to those observed for the virgin asphaltenes, indicating that the catalytic oxidation regime remains the same. However, an additional shoulder with a maximum at 460 °C is observed in this system. Such peak is also observable for MnO_2@HA and MnO_2@AA. The latter behavior suggests that under the studied conditions even under the presence of the solids, the asphaltenes might go under a noncatalytic route. This behavior might be due to the finite adsorption and the catalytic sites on the surface. The MnO_2 presents its maximum peak at 440 °C, whereas the functionalized materials exhibit peaks around 420–430 °C, indicating a nearly 60 °C reduction compared to the asphaltenes. This supports the notion that the metal oxide has catalytic activity and is not negatively affected by partial functionalization with carboxylic acids.

3.4.2. DSC analysis

Figure S5b (https://ejp.researchcommons.org/cgi/viewcontent.cgi?filename=0&article=1004&context=journal&type=additional&preview_mode=1) shows DSC analyzes of the virgin asphaltenes and asphaltene-impregnated functionalized materials. For virgin asphaltenes, the process is isothermal for temperatures up to 200 °C. However, for higher temperature at 400 °C, an exothermic profile is evidenced, and the analysis is similar for the DTA. In contrast, for MnO_2 catalytic systems, temperatures above 250 °C show that manganese dioxide is catalyzing the oxidation of asphaltenes[22] with an increase in heat flux due to the exothermicity of the process. In addition, the ignition temperature of the reactions is shifted to lower temperatures with the maximum peak at 340 °C compared to the system without catalyst at 450 °C.

Regarding MnO_2@HA and MnO_2@AA, an initial endothermic process is elucidated. The latter process might be related to the volatilization of light asphaltene fractions selectively adsorbed on the surfaces. Specifically, for MnO_2@AA the marked

endothermic peak around 337 °C is related to the vaporization of physisorbed molecules of the functionalization agent. However, the notable increase in heat flow per gram of asphaltenes in the samples changes drastically for temperatures above 200 °C. In fact, the maximum peak around 250 °C observed in all cases aligns with the LTO regime. Therefore, the functionalized materials show exothermicity at lower temperatures than MnO_2 and virgin asphaltenes; this finding is consistent with what was observed in DTG curves and TGA at temperatures below 350 °C. Hence, it can be inferred that Janus-type functionalization may have an effect on the catalytic activity of MnO_2 for asphaltene oxidation.

3.4.3. Activation energy calculation

The results obtained from the isoconversional OFW method are shown in Fig. 5. The graph shows progressive conversions up to 50%, corresponding to temperatures of ~450 °C for nanocatalyst and 470 °C for virgin asphaltenes which is consistent with the RTO results even when HTO reactions take place. The activation energy for the virgin asphaltenes is determined to be 290 kJ/mol, but it decreases to 200 kJ/mol as the conversion reaches 50%. This decrease in the activation energy as the conversion increases agrees with what was observed by Montoya et al.[8] affirming that the activation energy is not constant because the thermal cracking of asphaltenes is not a process depending on a single mechanism but rather on different reaction paths. However, the introduction of the catalyst modifies such behavior. Fig. 5 shows that before 40% conversion, both MnO_2 and its functionalized materials have lower activation energies than virgin asphaltenes, indicating an improvement in the catalytic process. This finding is in agreement with Galukhin et al.[23] where the presence of manganese ions decreases the activation energy of the heavy oil oxidation process, especially in the HTO region. In this work, the initial activation energy for the bare-MnO_2 is 50 kJ/mol which slightly increases up to a value of 73 kJ/mol for a conversion of 0.3.

The different trends observed for the activation energy versus conversion, increasing for MnO_2 and decreasing for the pure asphaltenes, suggest that different mechanisms are involved. For the virgin asphaltenes, the oxidation occurs in a homogeneous system meanwhile for the catalyzed system, the adsorption of the asphaltenes molecules takes places on the surface of the nanocatalyst prior oxidation.

Concerning JNMs, they exhibit a positive impact on activation energy. Furthermore, these materials present very similar values and follow the same trend, consistent with the characterization results, revealing similar physicochemical properties. Specifically, their activation energies fall within the range of 10–30 kJ/mol, notably lower than those observed for both asphaltenes and MnO_2.

Therefore, its improvement in the catalytic activity is supported. The decrease in the value of E_α means that less energy is necessary for the asphaltene oxidation reaction to be carried out. Furthermore, the Janus MnO_2 demonstrates greater catalytic

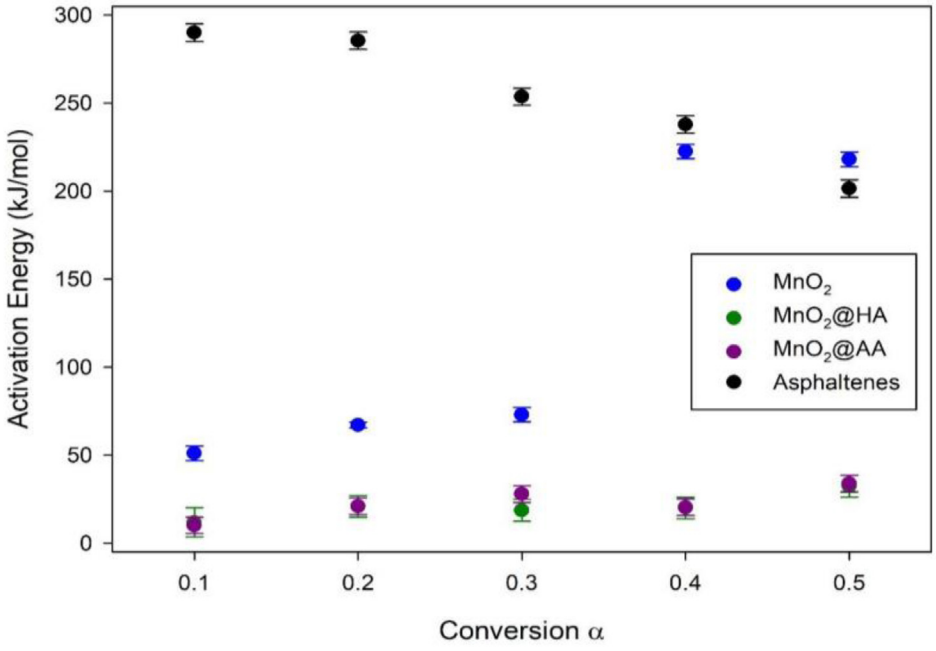

Fig. 5. Activation energy change with progressive conversion for OFW model. OFW, Ozawa–Flynn–Wall.

activity in accelerating combustion. This indicates that the functionalization with these organic molecules has a positive effect on the catalysis of MnO_2 in the oxidation of asphaltenes. Thus, the addition of acidic functional groups not only improves the stability of nanofluids but also kinetically favors the LTO and ITO-like reactions. Therefore, the enhanced catalytic activity of metal oxide nanomaterials, in terms of reducing the activation energy, is a function of the interaction between the nanoparticle surface and the asphaltene molecules.[24]

4. Conclusions

The synthesis of janus-type MnO_2 based nanomaterials was successful with the Pickering emulsion method. The functionalizing agents, that is, adipic and hexanoic acids, were capable of modifying the wettability and catalytic properties of the obtained materials. As a result, the stability of aqueous suspensions was significantly improved for the janus-type MnO_2-based nanomaterials compared to MnO_2 nanomaterials. This development in nanocatalyst transport during ISC holds significant promise. The addition of these carboxylic groups was evidenced mainly by TGA and SCA.

Regarding asphaltene-assisted combustion, all materials were impregnated with asphaltenes extracted from a heavy oil crude and analyzed by DSC technic; they showed catalytic properties, lowering the temperature of the asphaltene oxidation reaction.

Based on the research objective of evaluating the effect of anisotropic functionalization of JNM based on MnO_2 functionalized with adipic and hexanoic acid on the activation energy of the catalytic oxidation of asphaltenes at the LTO region using the OFW method, this study concludes that the anisotropic functionalization significantly reduces the activation energy. All materials exhibited decreased activation energy compared to virgin asphaltenes, at conversions below 40%. Moreover, the apparent activation energies for the functionalized materials are between 10 and 30 kJ/mol which is lower than bare MnO_2 (with activation energies between 50 and 230 kJ/mol). Subsequently, the addition of acidic functional groups not only improves the stability of nanofluids but also kinetically favors the LTO and ITO-like reactions. The lower activation energy indicates that the Janus catalyst enables the asphaltene oxidation reaction to occur more easily and at a faster rate compared to the unmodified MnO_2.

In general, all results suggest that the functionalization process with the studied organic molecules positively impacts on the transport and combustion (catalytic) process of heavy oil fractions such as asphaltenes, making it a potential candidate for improving the efficiency of asphaltenes oxidation in the LTO region.

Author contributions

P.A Rivera-Quintero: Investigation, Methodology, Investigation, Visualization, Writing—original draft and Writing—review & editing. **D. Fabio Mercado:** Conceptualization, Methodology, Verification, Formal analysis, Investigation, Supervision, Writing—review & editing, Supervision and Project administration. **Hernando Guerrero-Amaya**: Validation, Supervision. **Luz M. Ballesteros-Rueda:** Methodology, Verification, Formal analysis, Project administration, Writing—review & editing, Supervision and Funding acquisition.

Conflicts of interest

The authors declare that they have no known competing financial interests or personal relationships that could have appeared to influence the work reported in this paper.

Acknowledgements

The authors are grateful for the financial support of Ministerio de Ciencia, Tecnología e Innovación (Minciencias) of Colombia, and the Agencia Nacional de Hidrocarburos (ANH) of Colombia through Project number 44842-365-2018.

References

1. Olajire AA. Review of ASP EOR (alkaline surfactant polymer enhanced oil recovery) technology in the petroleum industry : prospects and challenges. *Energy*. 2014;77:963–982.
2. Guo K, Li H, Yu Z. In-situ heavy and extra-heavy oil recovery: a review. *Fuel*. 2016;185:886–902.
3. Kok MV, Keskin C. Comparative combustion kinetics for in situ combustion process. *Thermochim Acta*. 2001;369:143–147.
4. Castanier LM, Brigham WE. Upgrading of crude oil via in situ combustion. *J Pet Sci Eng*. 2003;39:125–136.
5. Mahdavi E, Zebarjad FS. Screening criteria of enhanced oil recovery methods. In: Bahadori A, ed. *Fundamentals of Enhanced Oil Gas Recovery from Conventional and Unconventional Reservoirs'. UK: G.P.P.* Elsevier Inc; 2018:41–60.
6. Wei B, Zou P, Zhang X, Xu X, Wood C, Li Y. Investigations of structure-property-thermal degradation kinetics alterations of Tahe asphaltenes caused by low temperature oxidation. *Energy Fuels*. 2018;32:1506–1514.
7. Zhao S, Pu W, Varfolomeev MA, et al. Comprehensive investigations into low temperature oxidation of heavy crude oil. *J Pet Sci Eng*. 2018;171:35–842.
8. Montoya T, Argel BL, Nassar NN, Franco CA, Cortés FB. Kinetics and mechanisms of the catalytic thermal cracking of asphaltenes adsorbed on supported nanoparticles. *Petrol Sci*. 2016;13:561–571.

9. Varfolomeev MA, Yuan C, Bolotov AV, et al. Effect of copper stearate as catalysts on the performance of in-situ combustion process for heavy oil recovery and upgrading. *J Pet Sci Eng*. 2021;207:109125.
10. Saifullin ER, Mehrabi-Kalajahi S, Yuan C, et al. Catalytic combustion of heavy crude oil by oil-dispersed copper-based catalysts: effect of different organic ligands. *Fuel*. 2022;316: 123335.
11. Golafshani MB, Varfolomeev MA, Mehrabi-Kalajahi S, et al. Oxidation of heavy oil using oil-dispersed transition metal acetylacetonate catalysts for enhanced oil recovery. *Energy Fuel*. 2021;35:20284−20299.
12. Li C, Huang W, Zhou C, Chen Y. Advances on the transition-metal based catalysts for aquathermolysis upgrading of heavy crude oil. *Fuel*. 2019;257:115779.
13. Amanam UU, Zeng H, Kovscek AR. Nanoparticle delivery to porous media via emulsions and thermally induced phase inversion. *Colloids Surf A Physicochem Eng Asp*. 2019;581: 123614.
14. Hashemi R, Nassar NN, Almao PP. Nanoparticle technology for heavy oil in-situ upgrading and recovery enhancement: opportunities and challenges. *Appl Energy*. 2014;133:374−387.
15. Mercado DF, Akimushkina L, Quintero PAR, Zapata RV, Amaya HG, Rueda LMB. Comprehensive analysis of the transition metal oxide nanomaterials role as catalysts in the low-temperature oxidation of adsorbed nC7-asphaltenes. *Fuel*. 2022;327:125179.
16. Quintero PAR, Mercado DF, Rueda LMB. Influence of the functionalization agent and crystalline phase of MnO2 Janus nanomaterials on the stability of aqueous nanofluids and its catalytic activity to promote asphaltene oxidation. *Colloid Interface Sci Commun*. 2021;45:100525.
17. Shi F, Wu J, Zhao B. Research on percolation characteristics of a JANUS nanoflooding crude oil system in porous media. *ACS Omega*. 2022;7:23107−23114.
18. Ghatee MH, Koleini MM, Ayatollahi S. Molecular dynamics simulation investigation of hexanoic acid adsorption onto calcite (1014)surface. *Fluid Phase Equil*. 2015;387:24−31.
19. Mercado DF, Weiss RG. Polydimethylsiloxane as a matrix for the stabilization and immobilization of zero⇑valent iron nanoparticles. Applications to dehalogenation of environmentally deleterious molecules. *J Braz Chem Soc*. 2018;29:1427−1439.
20. Penelas MJ, Soler-Illia GJAA, Levi V, Bordoni AV, Wolosiuk A. Click-based thiol-ene photografting of COOH groups to SiO2 nanoparticles: strategies comparison. *Colloids Surfaces A Physicochem Eng Asp*. 2019;562(2018):61−70.
21. Alhumaidan FS, Rana MS, Lababidi HMS, Hauser A. Pyrolysis of asphaltenes derived from residual oils and their thermally treated pitch. *ACS Omega*. 2020;5: 24412−24421.
22. Abu Tarboush BJ, Husein MM. Oxidation of asphaltenes adsorbed onto NiO nanoparticles. *Appl Catal. A General*. 2012; 445−446:166−171.
23. Galukhin A, Khelkhal MA, Gerasimov A, et al. Mn-catalyzed oxidation of heavy oil in porous media: kinetics and some aspects of the mechanism. *Energy Fuels*. 2016;30:7731−7737.
24. Nassar NN, Hassan A, Luna G, Pereira-Almao P. Kinetics of the catalytic thermo-oxidation of asphaltenes at isothermal conditions on different metal oxide nanoparticle surfaces. *Catal Today*. 2013;207:127−132.